FrontalPhotopolymerization of Fully Biobased Epoxy Composites

Frontal-photopolymerization of fully biobased epoxy composites

*Camilla Noè, Minna Hakkarainen,, Samuel Malburet, Alain Graillot, Kayode Adekunle, Mikael Skrifvars, Marco Sangermano**

C. Noè, M. Sangermano
Department of Applied Science and Technology, Politecnico di Torino, C.so Duca degli Abruzzi 24, 10129 Torino, Italy
M. Hakkarainen
Department of Fibre and Polymer Technology, KTH Royal Institute of Technology, Teknikringen 56-58, 10044 Stockholm, Sweden
S. Malburet, A. Graillot
Specific Polymers, 150 Avenue des Cocardieres, Castries 34160, France
K. Adekunle, M. Skrifvars
Swedish Centre for Resource Recovery, Faculty of Textiles, Engineering and Business, University of Borås, Allegatan 1, 501 90, Borås, Sweden

KEYWORDS: UV-curing, RICFP, biobased composite

The radical-induced cationic frontal photopolymerization (RICFP) of fully biobased epoxy composites is successfully demonstrated. This curing strategy considerably reducess the curing time and improves the efficiency of the composite fabrication. Two different natural fibre fabrics made of cellulose and flax fibres are embedded in two epoxy matrices, one derived from vanillin (diglycidylether of vanillyl alcohol-DGEVA) and the other from petroleum (3,4-epoxycyclohexylmethyl 3,4-epoxycyclohexanecarboxylate-CE). After RICFP the composites are characterized by means of dynamic mechanical thermal analysis and tensile tests. The mechanical properties improved with increasing fibre content, confirming a strong adhesion between the matrix and the reinforcing fibre fabrics, which is further evidenced by scanning electron microscopy analyses of the fracture surfaces. Furthermore, these fully bio-based composites possess comparable or even higher mechanical strength compared with the corresponding epoxy composites fabricated with conventional CE resin. A promising facile route to high-performing natural fibre-biobased epoxy resin composites is presented.

1. Introduction

Over the last years, fossil fuel depletion and the growing environmental concerns have driven researchers to the development of "green" biobased materials which are usually derived from biomass and/or are potentially biodegradable. Looking at polymers and composites, the substitution of petroleum-based materials represents a significant challenge [1]. Since 1990, many green composites made of natural reinforcement like vegetable fibres (kenaf, hemp, flax, and jute) embedded in fossil-fuel derived resins have been proposed as an alternative to conventional composites [2–12]. These natural fibres show higher specific strength and comparable Young's modulus with glass fibres [13]. Moreover, natural reinforcement possesses several other advantages over the synthetic fibre reinforcement since they are low cost and easy to process [4]. The main drawbacks of natural fibres are their hydrophilicity, the often-poor adhesion with the matrix and the variability of the properties due to the different growing plant factors [14,15]. Nevertheless, the achieved properties are enough to justify the usage of those composites in certain applications. Even if the use of natural reinforcements helps to reduce the CO_2 footprints, also the polymer matrix should be bioderived to obtain a fully biobased composite.

In recent years great attention has been given to the production of biobased thermoplastics (like starch [16,17] and polylactic acid [1,18,19]) reinforced with natural fibres (cellulose, bamboo, etc.). Those products can find their application as automotive parts, housing products and packaging [13]. Nonetheless, thermoplastic composites usually do not have sufficient strength, thermal, and chemical resistance to be used for structural or semi-structural applications such as construction, aerospace and aeronautics [20]. For those applications, the choice of highly crosslinked thermosets polymers is essential.

Among all the thermoset matrixes, epoxy resins are the most commonly used to obtain high-performance composites due to their strong adhesion to a broad range of substrates, superior mechanical properties, and high glass transition temperatures (over 100°C) [21,22]. The most used

biobased epoxy resins are vegetable oils (VOs), given their abundant availability and low cost. For this reason, many VO-based composites have been developed. For example, Shibata et al. successfully fabricated a microfibrillated cellulose composite using epoxidized soybean oil blended with tannic acid as a matrix [23]. However, the long aliphatic chains of VOs lead to the formation of flexible networks with low crosslinking density, resulting in composites with relatively poor mechanical properties [24].

To overcome this problem, different mixtures of VOs with petroleum-based resins have been proposed [22]. Sahoo et al., studied the properties of epoxidized linseed oil mixed with diglycidyl ether of bisphenol A (DGEBA) with sisal fibres [25], while Manthey et al. investigated a mixture of epoxidized hemp or soybean oils with diglycidyl ether-based epoxy resin using woven jute mat as reinforcement [14]. Alternatively, other partially biobased epoxidized resins can be currently found in the market like Super Sap™ [26–30] and System Bio Epoxy 01 S from ALPAS [31]. However, the bio-content of these commercial resins is generally quite low, ranging from 30 to 40%. Shibata et al. developed microfibrillated cellulose composites using glycerol polyglycidyl ether and sorbitol polyglycidyl ether resins cured with tannic acid [32], but in general very few works on biobased composites with high bio-epoxy content have been carried out.

It is important to point out that all the previously mentioned composites were obtained *via* conventional thermo-curing process, using expensive ovens or autoclaves. This process is mainly used in the manufacture of high-performing components for aerospace applications and requires rather much manual work. The thermo-curing process is also time-consuming and requires a large amount of energy, which is detrimental for a green economy. To overcome those drawbacks a new curing technique has been proposed in the last few years: the frontal polymerization technique (FP) [33–37]. Chechilo's group firstly described this innovative curing mechanism [38–41], based on the generation of a self-sustaining reaction front able to move through the whole sample. The heat released by the polymerization causes the decomposition

of a thermo-labile initiator, which starts a subsequent polymerization. However, the thermal front can only propagate if the amount of energy after the heat loss is enough to cleave the additional thermo-labile initiator. The FP technique can be divided into two categories according to the polymerization initiation mechanism: thermal or photo-induced. The photo-induced frontal polymerization technique can, in turn, be divided into two sub-categories according to the photopolymerization mechanisms: radical or cationic [42,43]. The cationic frontal photopolymerization, known as radical-induced cationic frontal polymerization (RICFP) technique, is very promising for curing thick epoxy samples, as already reported in the literature [44–46]. The mechanism involves the photo-cleavage of an iodonium salt which generates a superacid that can start the cationic ring-opening epoxy polymerization. The heat release will cleave the thermo-labile initiator generating reactive radicals, which are oxidized in the presence of iodonium salt, forming a reactive carbocation [47–49]. The first work on RICFP was reported by Mariani et al. In this work, a thick sample of 3,4-epoxycyclohexylmethyl 3,4-epoxycyclohexanecarboxylate (CE) resin was successfully cured with dibenzoyl peroxide and iodonium salt in the formulation [50]. Later, Crivello [51], Bomze et. al., [52], Klicovts et al. [53], and, Svajdlenkova et al. [54] further investigated this subject. All of them, however, used petroleum-based epoxy-resins.

The earliest attempts to produce RICFP composites were conducted on fillers dispersed in traditional epoxy resins. In 2016, Bomze et al. cured different mica composites with bisphenol-A diglycidylether (DGEBA) using 1,1,2,2-Tetraphenyl-1,2-ethanediol as thermal initiator and p(octyloxyphenyl)phenyliodonium hexafluoroantimonate as photoinitiator [55]. In 2017, Klikovitis et al. investigated the possibility to obtain epoxy-based composites reinforced with SiO_2 particles [56]. More recently, the use of multi-walled carbon nanotubes [57] and fumed silica [58] as reinforcement fillers for RICFP were also investigated. Spange et al. combined the RICFP of DGEBA with the radical polymerization of 2,2-spirobi[4H-1,3,2-benzodioxasiline] in a so-

called twin polymerization leading to the formation of nanostructured hybrid material composed of epoxy resin, phenolic resin and silicon dioxide [59].

Even if the RICFP of composites is attracting widespread interest, only a few works have been published up to now on fibre–reinforced composites (FRCs). The first papers concerning this subject were published by Sangermano et al., demonstrating successful fabrication of glass-fibre composites in 2018 [60] and carbon fibres epoxy composites in 2019 [61] though RICFP of a blend of bisphenol A (50–100%), bisphenol F (25–50%) and 1,6-hexanedioldiglycidylether (2.5–10%). Later, Tran et al. investigated the creation of RICFP DGEBA-based composites using different reinforcements including woven carbon fibres, glass microsphere, graphite and aluminium [62]. Tran et al. reported the development of carbon fibre prepreg using a dual curing system consisting of 1,6-hexanediol diacrylate (HDDA) and DGEBA. The prepreg was obtained by radical polymerisation of HDDA, which does not affect the epoxy-ring reaction. The composite could be obtained in a second time by activating the RICFP of the DGEBA [63]. However, the applicability of RICFP on fully biobased natural fibre composite systems is still to be demonstrated. To fill this gap, we investigated the RICFP of an epoxidized vanillin-resin matrix reinforced with either linen or cellulose fabrics. As a comparison, the RICFP of a well-established radical-induced cationic frontal polymerizable petroleum-based resin: (CE) [64,65] reinforced with the same biobased fabrics was performed and RICFP process and final properties of the fabricated composites were evaluated and compared.

2. Results and discussion

Fully biobased epoxy-cellulose and epoxy-linen composites were fabricated *via* UV-activated RICFP. Vanillyl alcohol was epoxidized by means of hydroxyl group substitution to make it photocurable, following a two-step one-pot process (**Scheme 1**) already reported in previous works [66,67] and fully described in the experimental section. In Scheme 1 is reported an example

of DGEVA monomer structure, which may vary depending on which alcohol group the epichlorohydrin reacts with.

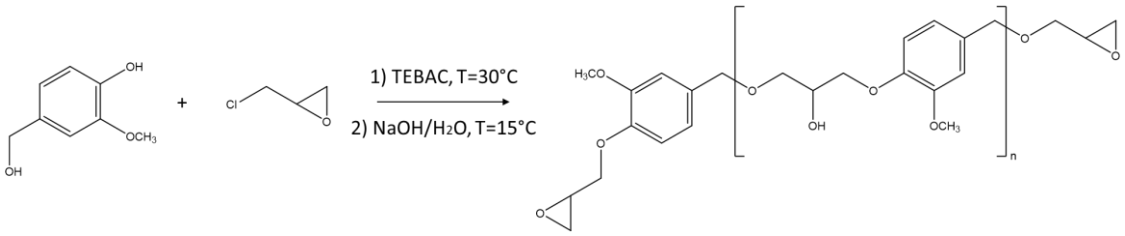

Scheme 1. Reaction scheme for epoxidation of vanillyl alcohol with an example of a possible DGEVA structure.

The success of the epoxidation reaction was confirmed by NMR spectroscopy, where the typical signals of epoxy ring protons (δ^1= 2.64, 2.82, and 3.21) and R-CH_2-O protons (δ^1= 3.42 and 3.75) can be clearly seen in the ^{1}H spectrum of DGEVA. The determination of the epoxy value was carried out by NMR titration. The calculated epoxy index was 7.28 m_{eq}/g and the estimated average number of repeating units was n=0.03 [67].

The radical-induced cationic frontal photopolymerization mechanism involves as a first step UV-irradiation which initiates the highly exothermic opening of the epoxy rings. Subsequently, the heat released starts the frontal polymerization by inducing the dissociation of the radical thermal initiator. The generated carbon-centred radicals are oxidized to carbocations, in the presence of the iodonium salt [44,68], which further propagates the cationic ring-opening polymerization towards the thickness of the samples until the sustainability of the front heat. The reaction mechanism is reported in **Scheme 2**.

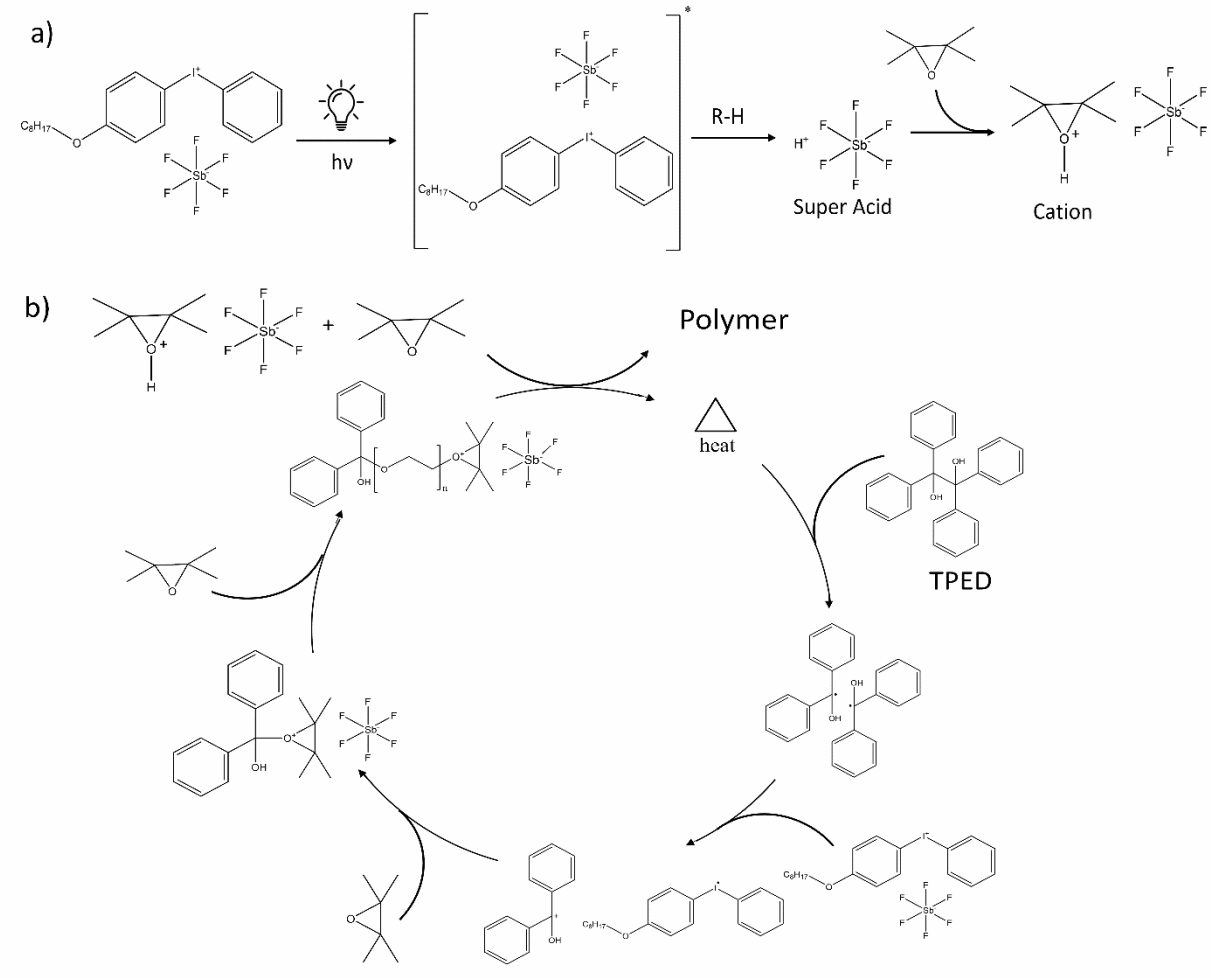

Scheme 2. (a) Light induced decomposition of a diphenyliodonium salt (PAG) and subsequently photoacid generation (b) epoxy ring-opening with heat generation and reaction propagation with the radical formation of the C-C labile compound of (1,1,2,2-tetraphenyl-1,2-ethanediol TPED (thermal) initiator.

Aiming at successful fabrication of fully cured composites, the heat dissipation due to the presence of the fibres must be considered, since the thermal-front propagation requires a constant heat generation. Preliminary experiments were conducted with the pristine formulations to find the optimum photoinitiator-thermal initiator concentration needed to generate a self-sustaining heat front and maximize the epoxy-group conversion. Fulfilling the

above-mentioned requirements, the formulation containing 1 %wt/1 %wt TPED/PAG was selected for further investigations of the frontal polymerization of the composites. The polymerization front was monitored using a thermal camera. **Figure 1(a)** illustrates schematically the photo-initiated thermal front propagation process, while **Figure 1(b)** displays corresponding images of the photo-initiated thermal propagation of pristine DGEVA formulation extracted from the movie recorded with the thermo-camera (See experimental section).

The front parameters namely 1) front starting time (t_0), 2) front velocity (V_f), and 3) maximum front temperature (T_{max}), of DGEVA and DGEVA composites are reported in **Table 1**. Thethermal front propagation velocity was calculated from the temperature profile registered atthree different points of the sample (X=10, 20 and 50 mm) (**Figure 1(c); Figure 2**), monitoring the time in which the T_{max} is reached [69]. An enhancement of starting time and a slight increase of the V_f was observed for both fibre composites with respect to the DGEVA pristine formulation. This result can be ascribed to the good thermal conductivity of the fibres, as already reported in previous works [70,71]. Remarkably, the V_F value for DGEVA is higher than the ones reported in the literature for others RICFP petroleum-based epoxy resin formulations [54,55,72].

The thermal front propagated at a constant rate with a linear behaviour (**Figure 1(d)**). This strongly supports the hypothesis of a front propagation mechanism. From the T_{max} values, reported in **Table 1**, it is evident that the thermal fronts reached a very high temperature, up to 285°C, similar to the values previously reported for the RICFP of DGEBA with TPED and PAG (283°C) [54].

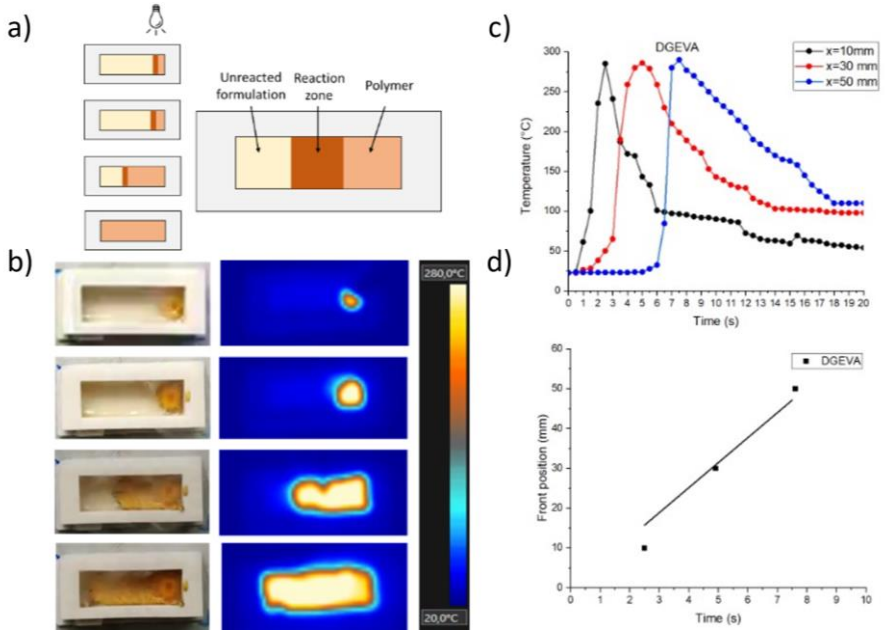

Figure 1. (a) schematic presentation of the photo initiated thermal front; (b) thermo-camera frame sequence of the propagating DGEVA thermal front; (c) temperature-time evolution at three different DGEVA specimen positions; d) DGEVA front position as a function of time.

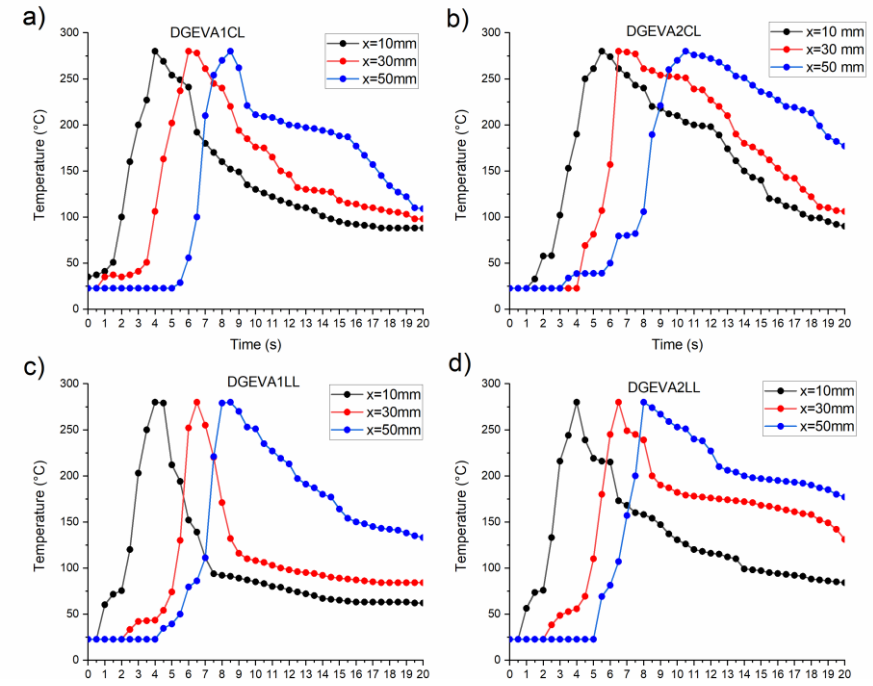

Figure 2. temperature–time evolution at three positions along the composites from the trigger point of (a) DGEVA1CL, (b) DGEVA2CL, (c)DGEVA1LL and (d) DGEVA2LL.

To investigate the photo-crosslinking reaction of the DGEVA resin, FTIR transmission spectra were recorded before and after RICFP curing (**Figure 3**). The two intense peaks at 2930 and 2970 cm^{-1} can be attributed to the sp^3 C-H bond vibration of the aliphatic chain [73], while the small ones at 3000 and 3060 cm^{-1} can be assigned to the methyl groups close to the epoxy rings [74]. The band at 1600 cm^{-1} corresponds to the C-O vibration, while the vanillyl fingerprint region is located between 1261 to 1160 cm^{-1}. The peaks centred at 1230 and 1260 cm^{-1} represent $-CH_2$ twisting and wagging vibrations respectively. The peaks ranging from 1453 to 1592 cm^{-1} can be assigned to the C=C vibration of the substituted benzene [75].

The success of the RICFP was confirmed by the decrease of peaks centred at 850-800 cm^{-1} and 910 cm^{-1}, corresponding to the characteristic vibration of the epoxy rings. Moreover, a broad peak centred at 3460 cm^{-1} appeared after the curing, as expected since the opening of the epoxy rings leads to the formation of hydroxyl groups [76,77]. The epoxy ring conversion (82%) was calculated by measuring the decrease of the epoxy ring peak centred at 910 cm^{-1}, as described in the experimental section.

DSC-dynamic thermograms were also recorded on the DGEVA pristine formulations. The area under the exothermic peak can be used to calculate the epoxy group conversion. As shown in the DSC-dynamic thermograms (**Figure 1S**), an exothermic peak can be observed at 120°C with a heat release of 129.44 J/g. This value can be attributed to the total epoxy group conversion. The exothermal response entirely disappears in the second thermal scan performed on the sample, where instead, a glass transition temperature (Tg) of about 75°C can be observed. Whereas, only a weak exothermal signal with an exothermicity of 3.18 J/g can be seen in the DSC thermogram of the RICFP cured polymer. This signal can be associated with residual thermal polymerization and it is absent in the second heating scan. From the obtained exothermicity values the epoxy group conversion during RICFP reaction was estimated to be around 90% for the pristine DGEVA formulation. The higher epoxy group conversion obtained by the DSC analyses with respect to the FTIR measurements could be explained by considering

the non-negligible heat loss to the surrounding that occurred during the curing of the FTIR samples.

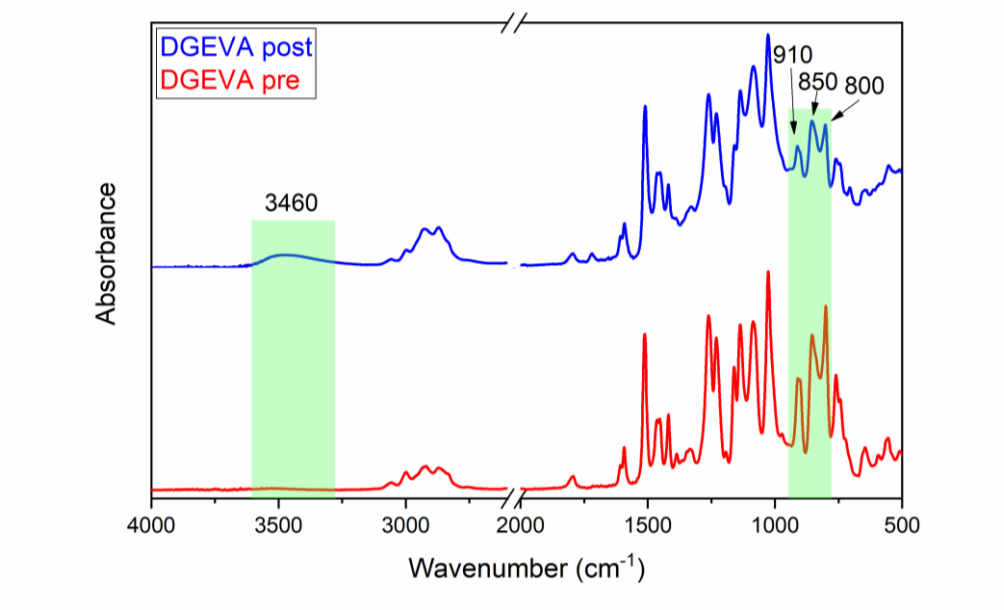

Figure 3. FTIR spectra of the DGEVA pristine formulation on silicone substrate pre and post curing. Film thickness 12 µm.

However, it was not possible to calculate a quantitative epoxy group conversion from the FTIR analysis on composites specimens since the thickness was too high for a transmission analysis and from the ATR-FTIR spectra of the cured samples it is only possible to obtain qualitative information.

Therefore, the efficiency of the curing was evaluated by calculating their gel or insoluble fraction contents (Gel%) (**Table 1**). The obtained Gel% values are always higher than 95%, which suggests a highly efficient curing reaction with a minor amount of not fully cured extractables.

Table 1. Thermal-front parameters.

	t_0 [s]	V_f [cm min^{-1}]	T_{max} [°C]	%Gel
DGEVA	2	48±2	280±4	96±2
DGEVA1CL	4	69±4	285±2	96±1
DGEVA2CL	5	66±2	278±1	98±1

DGEVA1LL	4	67±4	285±2	95±2
DGEVA2LL	4	62±3	277±3	96±2

The thermo-mechanical and tensile properties of the prepared fully biobased composites were analysed by means of DMTA and tensile test measurements. All the tests were also conducted on RICFP cured CE composites made with the same fibres to make a comparison with a commercially-available petroleum-based resin..

The DMTA analysis allows evaluation of the viscoelastic properties of the material, giving information on the storage and loss moduli (elastic component-E' and viscous component-E'' respectively). The E'' is a measure of the energy dissipated in the material. The maximum of the damping factor curve (E''/E', commonly known as Tanδ), was used to estimate the glass transition temperature (Tg) of the composites.

The averaged Tanδ (E''/E') and the storage modulus (E') plots of the pristine DGEVA and CE thermoset resins and their cellulose and linen composites are shown in **Figure 4.** As can be noted, the Tanδ maximum shifted towards higher temperature and the E' values increase with the addition of the fibre fabrics indicating a good stress transfer between the matrix and the fibres so an effective reinforcement of the thermoset matrix. In fact, the E' in composites increases when the polymer chains movements are hindered by fibre-fibre and fibre-matrix interactions [78]. The presence of the fibres lowered the Tanδ peak of the DGEVA composites, this can be ascribed to the reinforcement effect of the fibres, which reduces the mobility of the polymer chains, lowering the damping factor [79]. However, this Tanδ behaviour is not so evident in the CE composites presumably caused by a less homogeneous network formation and by a decrease of interfacial bonding [80]. Remarkably, the addition of flax fibres results in an enhancement of the Tg, which is more evident in the DGEVA composites (91 - 130°C) with respect to the CE ones (93 - 107°C). This result can be explained by considering a lower interfacial interaction between CE and flax fibres. Moreover, it can be observed that the Tanδ curves of the CE-cellulose composites **(Figure 4(d))** remained almost unchanged with the

addition of the fibres while the Tanδ of the CE-linen composites **(Figure 4(c))** shifts towards higher temperature. This may suggest a different interaction between those two types of fibres fabrics and the CE matrix. Nevertheless, an increase in the E‘ modulus was observed with increasing content of fibres independently from the matrix being used. Therefore the Tanδ behaviour of the CE-cellulose composites can be explained considering an enhancement in the energy dissipation (E‘‘) which can be ascribed to: weak interfaces adhesion between the CE and the cellulose fibres, weak bonds between neighbouring fibres or a shear stress concentration between fibres close to each other [81].

For all the composites studied, the E’ values decreased as the temperature increased, which can be attributed to the softening of the polymer matrix at high temperatures. The DGEVA composites showed noteworthy high glass transition temperatures (104 -143°C) and excellent storage modulus values (54-130 MPa). Interestingly, the storage modulus values of DGEVA composites are similar to those of petroleum-based CE composites.

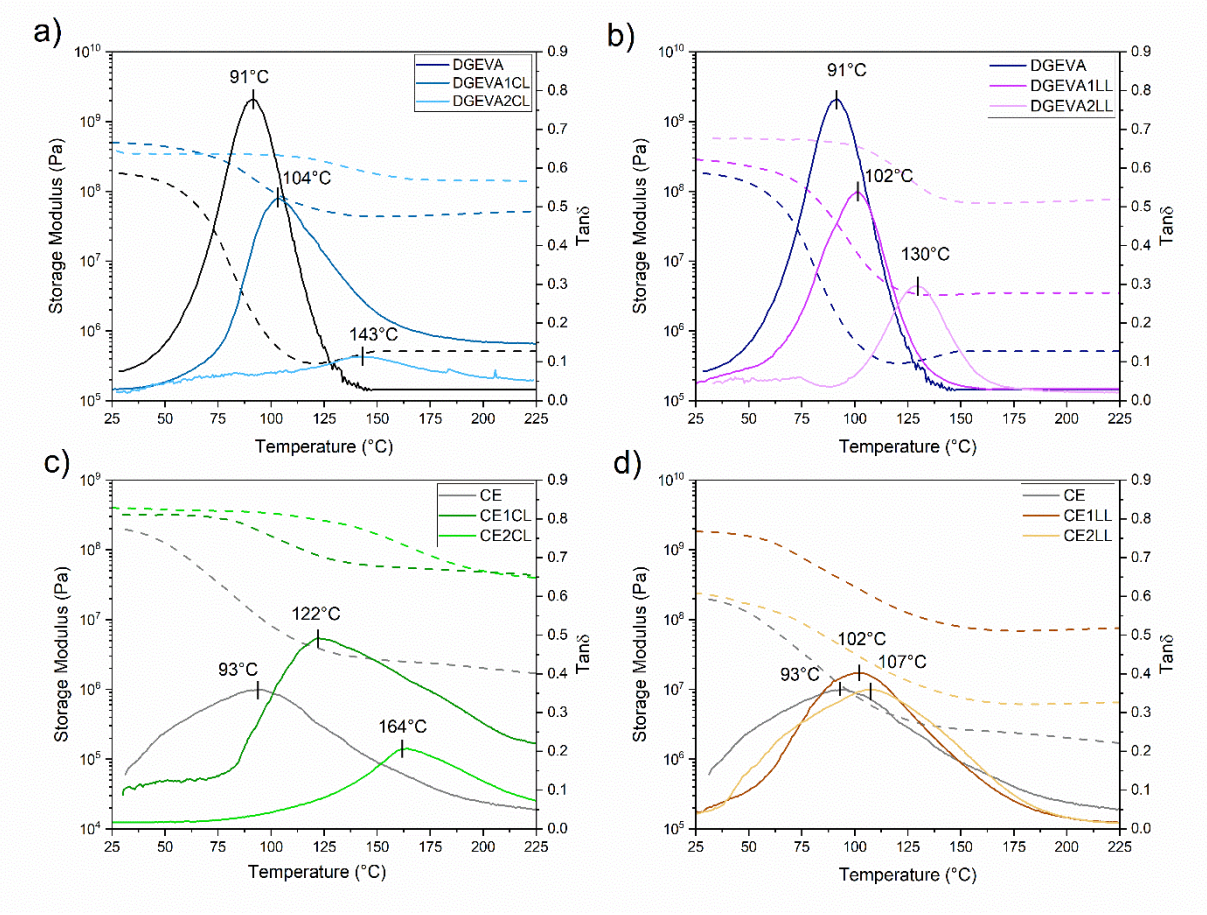

Figure 4. Tan δ and storage modulus curves of crosslinked epoxy–cellulose (right) and epoxy-linen (left) composites. (a) DGEVA-cellulose, (b) DGEVA-linen, (c) CE-cellulose and (d) CE-linen.

The averaged tensile stress-strain curves of the fibre-reinforced composites are reported in **Figure 5**. A slight enhancement of the elongation at break with respect to the pure resin can be seen for all the composites, except for the DGEVA1CL, suggesting a small increase of ductility as compared to the brittle pristine resins (**Figure 5**). Overall, the addition of the fibres on the polymeric matrix enhanced the mechanical strength of the composites, in accordance with the mechanical reinforcement trend observed in the DMTA analysis. These results further confirmed that the fibres act as an effective reinforcement agent, further suggesting strong adhesion between the matrix and the fibres.

The unidirectional non-woven cellulose DGEVA composites (**Figure 5(a)**) turned out to be stiffer and more brittle than the woven flax DGEVA composites (**Figure 5(c)**) due to a lower elongation at break and a higher tensile strength. This behaviour can be ascribed to the interlocking effect of warp and fill yarn [82].

The Young's modulus values were calculated from the slope of the initial linear region of the stress-strain curve (**Figure 6**). Remarkably, even if the rigidity of the pristine DGEVA was lower than the CE crosslinked network, the DGEVA composites show comparable or even Young's modulus values with respect to the corresponding petroleum-based resin composites. The DGEVA cellulose and DGEVA linen composites achieved maximum Young's modulus (E) of 1.2 GPa and 0.8 GPa respectively. This can be compared to Young´s modulus values of 0.8 and 0.6 GPa for the corresponding CE composites, respectively. The maximum tensile strength (σ_{max}) values ranged from 10 to 18 MPa for the cellulose composites and from 6 to 12 MPa for the linen composites **(Figure 6**). The maximum tensile strength values for the petroleum-based CE composites ranged from 11 to 17 MPa for cellulose composites and 6 to 7 MPa for linen composites. The obtained E and σ_{max} values of the fabricated vanillin-based composites are also in the same order of magnitude than those reported in the literature for other natural-fibres reinforced epoxy composite, but the curing time is markedly lower (**Table 2**). Moreover, all the specimens exhibited very low elongation at break values, as can be expected for fibre reinforced composites.

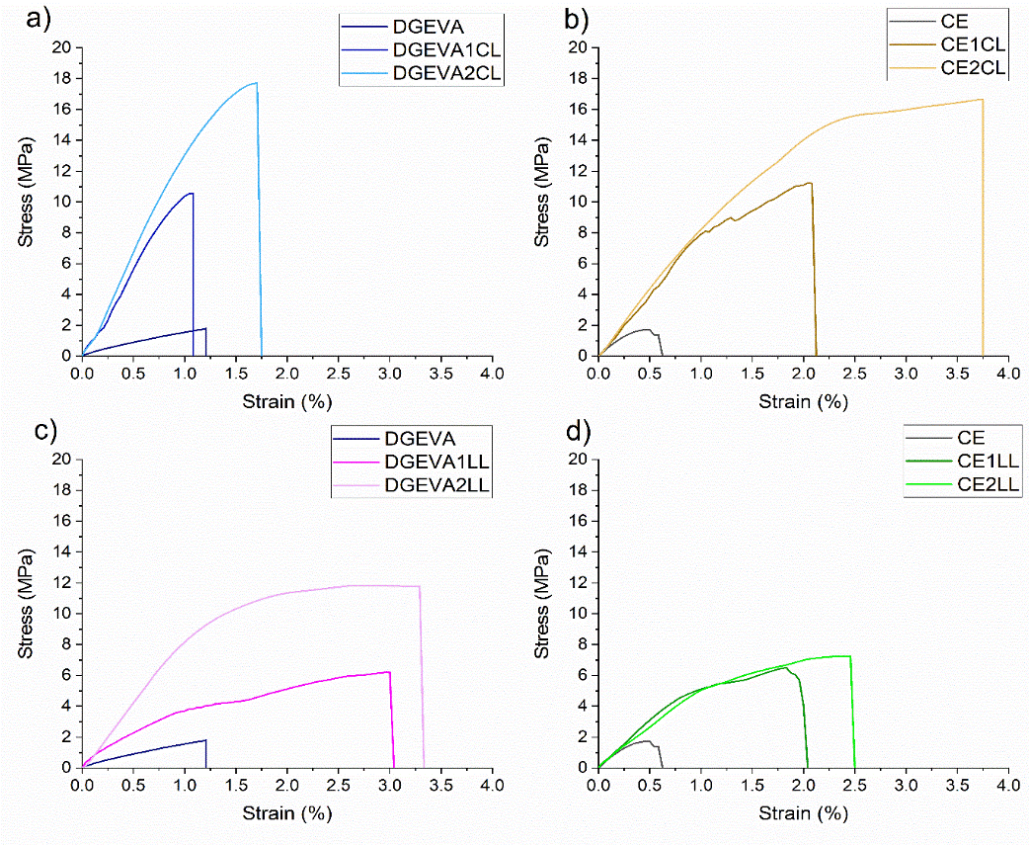

Figure 5. Stress-Strain curve of DGEVA composites (a, c) and CE composite (b, d).

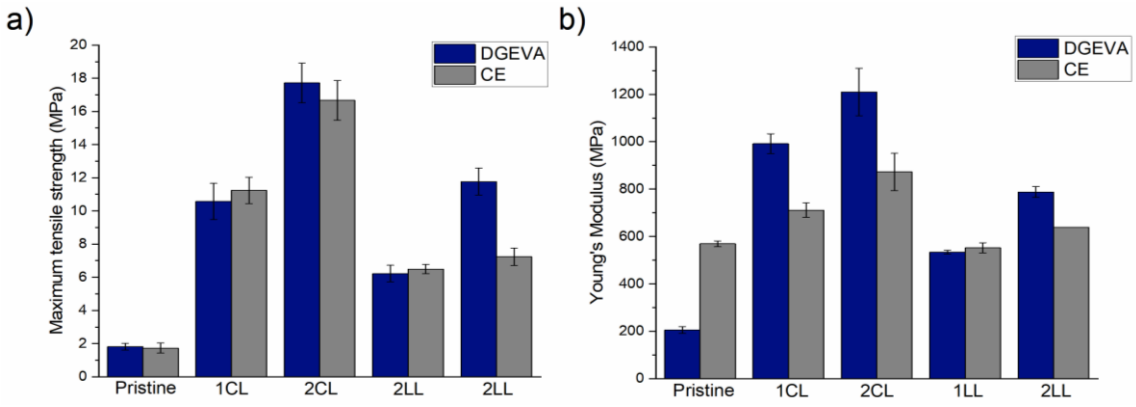

Figure 6. Comparison of a) maximum tensile strength and b) Young's modulus between DGEVA and CE composites.

Table 2. Tensile properties of similar natural fibre reinforced composites reported in literature compared with the properties achieved by the composites prepared with RICFP in present work.

Type of curing	Fibre reinforcement	Curing time	Tensile strength [MPa]	Young's Modulus [MPa]	Reference
Thermal	Kenaf/glass	/	40-110	6000-1200	[83]
Thermal	Kenaf	/	25-40	3000-5000	[84]
Thermal	Jute/hemp/flax	24 h	30-60	1000-1700	[85]
Thermal	Aloevera and sisal	24 h	19-27	/	[86]
Thermal	Jute/pineapple and glass	24 h	40-70	500-900	[83]
Thermal	Coir/glass fibre	24	30-60	/	[87]
Thermal	Pineapple/flax	/	22-35	/	[88]
RICFP	Cellulose/linen	1 min	6-18	600-1200	*Present work

Scanning electron microscopy (SEM) was used to investigate the morphologies of the cross-linked composites and the fibre-matrix adhesion. SEM images of the fracture surfaces of the DGEVA epoxy composites are displayed in **Figure 7**. As can be seen from the images, the resin diffused inside the yarn suggesting good wettability of both fibre fabrics with DGEVA. This results in a strong adhesion with the DGEVA matrix, in good agreement with the data obtained from the tensile tests. It can also be noticed that the failure mechanism involved in the composites after the tensile breakage is a mixture of fibre debonding and fibre pull-out which are key damage mechanisms in fibre loaded composites.

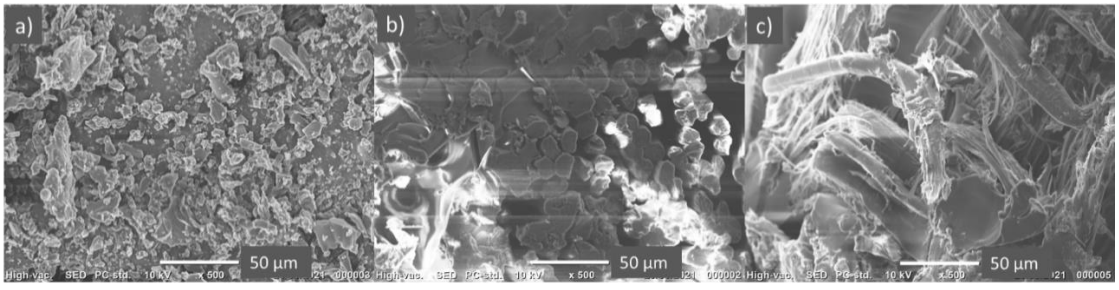

Figure 7. SEM images of the fracture surfaces of a) pristine DGEVA, b) DGEVA1CL and d) DGEVA1L.

3. Conclusions

The applicability of RICFP for the preparation of fully biobased epoxy natural fibre composites was successfully demonstrated. The biobased thermoset matrix was synthesized by epoxidation of vanillin alcohol. Cellulose and flax fibres were selected as biobased reinforcement. The RICFP of the biobased epoxy natural fibre composites showed high front velocity. Moreover, compared to the more conventional thermo-curing process the RICFP lead to a striking reduction of processing time. The successful curing was illustrated by the high, up to 96%, epoxy group conversion of the vanillin resin. The fibre-matrix composites exhibited good thermo-mechanical properties with glass transition temperatures ranging from 104 to 143°C and from 102 to 130°C, when cellulose and linen fabric were used as reinforcement, respectively. The biobased epoxy thermoset composites showed similar or even improved tensile mechanical properties compared to the corresponding petroleum-based CE thermosets, with Young's modulus and maximum tensile strength ranging from 600 to 1200 MPa and 6-18 MPa, respectively. Moreover, these mechanical properties match the values reported in the literature for other natural-fibres reinforced composites prepared from petroleum-derived epoxy resins. Both the thermo-mechanical and mechanical properties, including storage modulus, Young's modulus and tensile strength, of the composites, increased with the increasing fibres fraction content, indicating good adhesion between the thermosets and the fibres, as further confirmed by SEM analyses. These results provide compelling evidence for the feasibility of using biobased matrixes for fast, energy-efficient production of high-performance composites *via* RICFP.

4. Experimental Section

Materials

Diglycidylether of vanillyl alcohol (DGEVA), used as biobased epoxy monomer, was synthetized and provided by Specific Polymers. 3,4-Epoxycyclohexylmethyl 3,4-

epoxycyclohexanecarboxylate (CE), selected as petroleum-based epoxy resin, the 1,1,2,2-tetraphenyl-1,2-ethanediol (TPED) as thermal initiator were purchased from Sigma Aldrich. The cationic photoinitiator: (p-octyloxyphenyl)phenyliodonium hexafluoroantimonate (PAG) was obtained from ABCR. Vanillyl alcohol (98%), epichlorohydrin, benzyltriethylammonium chloride (TEBAC) (99%), anhydrous sodium sulphate Na_2SO_4 (99%), sodium hydroxide pellets (NaOH) and all solvents (> 95%) used were purchased from Sigma Aldrich. The fabric mats: cellulose unidirectional non-woven fibres, and woven flax fibres (linen) were supplied by HP Johannesson Trading AB, Sweden. All the chemicals were used as received.

2.2 Synthesis of diglycidylether of vanillyl alcohol (DGEVA)

DGEVA was synthetized as previously reported [67,89]. Accordingly, 10 g of vanillin alcohol and 1.5 g of benzyltriethylammonium chloride were mixed together. Subsequently, 60 g of epichlorohydrin was added and the solution was heated at 30°C for 4 h with stirring. Then, the mixture was cooled down to 15°C and NaOH (33 %wt) solution was slowly added. The reaction was left to react overnight at 15°C, after which deionized water and ethyl acetate were added. The organic layer was washed two times with deionized water and dried with anhydrous Na_2SO_4. A rotary evaporator was used to remove the remaining traces of solvents.

2.3 Biobased composite preparation

Thermoset composites were prepared with either cellulose fabrics or the linen fabrics as fibre-reinforcement. Neat DGEVA was mixed with 1 phr (parts per hundred resin) of TPED and 1 phr of $Ph_2I^+SbF_6^-$ (PAG). To ease the photoinitiator dissolution it was dissolved in propylene carbonate (50:50 wt%). Different samples (10x50 mm, thickness 2 mm) were prepared by impregnating one cellulose (DGEVA1CL), one linen (DGEVA1LL), two cellulose (DGEVA2CL) or two linen (DGEVA2CL) plies of fibres. After 30 minutes of vacuum impregnation, the corner of the mould was irradiated with UV lamp (Light-Ning Cure™ LC8, Hamamatsu) equipped with an optical fibre for 1ss, to activate the thermal front. For comparison composites made by CE as a petroleum-based epoxy matrix with the same fibres

ratio were also prepared and cured under the same conditions and with the same TPED/PAG system. All the composite compositions are reported in **Table 3**.

Table 2. Composite compositions.

	PAG (phr)	TPED (phr)	N° Cellulose layers	N° linen layer
DGEVA	1	1	/	/
DGEVA1CL	1	1	1	/
DGEVA2CL	1	1	2	/
DGEVA1LL	1	1	/	1
DGEVA2LL	1	1	/	2
CE	1	1	/	/
CE1CL	1	1	1	/
CE2CL	1	1	2	/
CE1LL	1	1	/	1
CE2LL	1	1	/	2

Characterization

Proton nuclear magnetic resonance (^{1}H-NMR)

^{1}H-NMR spectrum of the synthesized monomer was obtained using Bruker Advance 300 (300 MHz) spectrometer equipped with a QNP probe at room temperature (RT). DGEVA was solubilized in $CDCl_3$-d6.

Fourier transform infrared spectroscopy (FTIR)

The FTIR spectra of DGEVA before and after photocrosslinking reaction were recorded by Nicolet iS 50 Spectrometer. The samples were scanned from 4000 to 500 cm^{-1} with 4 cm^{-1} resolutions. Data were recorded and processed using the software Omnic from Thermo Fisher Scientific. The epoxy conversion was calculated by following the decrease of the peak centred at 910 cm^{-1}. To quantify this variation, the peak at 1511 cm^{-1} representing the C=C bond stretching vibration of the aromatic ring was taken as internal standards, since it is not affected by the reaction. The calculation was done following the **Equation 1**.

$$Conversion(\%) = \left(1 - \frac{\frac{A_{epoxy\_post}}{A_{epoxy\_pre}}}{\frac{A_{ref\_post}}{A_{ref\_pre}}}\right) * 100 \quad (1)$$

Where A_{epoxy_pre} and $A_{epoxy\text{-}post}$ are the area of the epoxy peak before and after the frontal polymerization respectively. While $A_{ref\text{-}pre}$ and $A_{ref\text{-}post}$ are the area of the reference signal before and after the fontal polymerization respectively.

Frontal polymerization evaluation

The set up for the evaluation of the RICFP front consists of a silicon mould for the polymerization (10 mm x 50 mm, thickness 3 mm), an optic fibre UV-light irradiation for the reaction initiation (Hamamatsu LC8 lamp, 100 mW/cm^2), and a thermo-camera for the evaluation of the front characteristics (FLIR E5, with a thermal sensibility of 0.1 °C and an IR resolution of 10,800 pixels). The thermo-camera was set to register the temperature of a single spot (chosen accordingly to the specimen position desired) at different time intervals. The experiments were repeated in triplicates.

Gel content % (G%)

The gel content percentage (G%) of the cured composite was determined by measuring the weight loss after 24 h extraction with chloroform at RT. G% was calculated according to **Equation 2**:

$$G\% = \frac{W_i}{W_0} x\ 100\% \qquad (2)$$

where W_i is the weight of the dry composite after the treatment in chloroform and W_0 is the weight of the dry sample before the treatment.

Differential scanning calorimetry (DSC)

DSC analysis were performed by using a Mettler Toledo DSC instrument. Samples having masses of approximately 6 mg were inserted in 100 µl aluminium pans with pierced lids in a nitrogen atmosphere. The applied heating rate was 10 °C min^{-1} in a nitrogen atmosphere (rate 50 ml min^{-1}). The thermal behaviour of the samples was investigated using the following two heating/cooling cycles from 25 to 200°C.

Dynamic mechanical-thermal analysis (DMTA)

DMTA experiments were performed with a Triton Technology instrument. Measurements were run in triplicates from 25 to 250°C with a heating rate of 3 °C min^{-1} in an oscillatory tensile mode. The displacement was set at 0.02 and the frequency at 1Hz.

Tensile Test

Tensile tests were performed according to ASTM D3039 [90] using MTS QTestTM/10 Elite controller (MTS Systems Corporation, Edan Prairie, Minnesota, USA) and TestWorks® 4 software (Edan Prairie, Minnesota, USA). The cross-head displacement rate was set at 2 mm/min. The experiments were conducted in triplicates. The Young's modulus (E) was calculated from the initial slope of the stress–strain curve. The tensile strength and elongation at break were calculated as the maximum stress value in the stress-strain curve.

Scanning Electron Microscopy (SEM)

The morphological characterization of the composites was performed by using a SEM (JCM-6000PLUS, JEOL). The tensile-fractured samples were covered with 5 nm thick film of platinum and observed with the microscope.

Supporting Information

Supporting Information is available from the Wiley Online Library or from the author.

Acknowledgements

Camilla Noè: Methodology, Investigation, Writing - Original Draft. Samuel Malburet and Alain Graillot: synthesis of diglycidylether of vanillyl alcohol. Kayode Adekunle and Mikael Skrifvars supplied the fabric mats. Minna Hakkarainen review & editing, Supervision, Marco Sangermano: Conceptualization, review & editing, Supervision.

Received: ((will be filled in by the editorial staff))
Revised: ((will be filled in by the editorial staff))
Published online: ((will be filled in by the editorial staff))

References

1. J. F. Balart, V. Fombuena, O. Fenollar, T. Boronat, L. Sánchez-Nacher, *Composites Part B: Engineering* **2016**, *86*, 168.
2. C. Scarponi *et al.*, *Composites Part B: Engineering* **2016**, *91*, 162.
3. L. Sobczak, R. W. Lang, A. Haider, *Composites Science and Technology* **2012**, *72*, 550.
4. S. v. Joshi, L. T. Drzal, A. K. Mohanty, S. Arora, *Composites Part A: Applied Science and Manufacturing* **2004**, *35*, 371.
5. L. Sobczak, R. W. Lang, A. Haider, *Composites Science and Technology* **2012**, *72*, 550.
6. S. Alsubari *et al.*, *Polymers* **2021**, *13*, 423.
7. S. Vigneshwaran *et al.*, *Journal of Cleaner Production* **2020**, *277*, 124109.
8. S. C. Chin, K. F. Tee, F. S. Tong, H. R. Ong, J. Gimbun, *Materials Today Communications* **2020**, *23*, 100876.
9. M. Li *et al.*, *Composites Part B: Engineering* **2020**, *200*, 108254.
10. A. Gholampour, T. Ozbakkaloglu, *Journal of Materials Science* **2020**, *55*, 829.
11. Z. Zhang *et al.*, *Composites Science and Technology* **2020**, *194*, 108151.
12. K. R. Sumesh, K. Kanthavel, V. Kavimani, *International Journal of Biological Macromolecules* **2020**, *150*, 775.
13. A. K. Mohanty *et al.*, **2005**, doi:10.1201/9780203508206.
14. N. W. Manthey, F. Cardona, G. Francucci, T. Aravinthan, *Journal of Reinforced Plastics and Composites* **2013**, *32*, 1444.
15. Y. Xu, K. Adekunle, S. K. Ramamoorthy, M. Skrifvars, M. Hakkarainen, *Composites Communications* **2020**, *22*, 100536.
16. A. A. S. Curvelo, A. J. F. de Carvalho, J. A. M. Agnelli, *Carbohydrate Polymers* **2001**, *45*, 183.
17. R. Jumaidin, N. A. Diah, R. A. Ilyas, R. H. Alamjuri, F. A. M. Yusof, *Polymers* **2021**, *13*, 1420.
18. M. R. Nurul Fazita *et al.*, *Materials* **2016**, *9*, 435.
19. B. Baghaei, M. Skrifvars, *Composites Part A: Applied Science and Manufacturing* **2016**, *81*, 139.
20. E. Ramon, C. Sguazzo, P. Moreira, *Aerospace* **2018**, *5*, 110.
21. F. Ferdosian, Y. Zhang, Z. Yuan, M. Anderson, C. (Charles) Xu, *European Polymer Journal* **2016**, *82*, 153.
22. L. di Landro, G. Janszen, *Composites Part B: Engineering* **2014**, *67*, 220.
23. M. Shibata, N. Teramoto, K. Makino, *Journal of Applied Polymer Science* **2011**, *120*, 273.
24. X. Q. Liu, W. Huang, Y. H. Jiang, J. Zhu, C. Z. Zhang, *Express Polymer Letters* **2012**, *6*, 293.
25. S. K. Sahoo, V. Khandelwal, G. Manik, *Polymer Composites* **2018**, *39*, E2595.
26. T. Scalici, V. Fiore, A. Valenza, *Composites Part B: Engineering* **2016**, *94*, 167.
27. S. Wang, R. Masoodi, J. Brady, B. R. George, *Journal of Renewable Materials* **2013**, *1*, 279.

28. H. N. Dhakal, Z. Y. Zhang, N. Bennett, A. Lopez-Arraiza, F. J. Vallejo, *Journal of Composite Materials* **2014**, *48*, 1399.
29. R. Masoodi, R. F. El-Hajjar, K. M. Pillai, R. Sabo, *Materials and Design* **2012**, *36*, 570.
30. B. Barari *et al.*, *Carbohydrate Polymers* **2016**, *147*, 282.
31. L. di Landro, G. Janszen, *Composites Part B: Engineering* **2014**, *67*, 220.
32. M. Shibata, K. Nakai, *Journal of Polymer Science, Part B: Polymer Physics* **2010**, *48*, 425.
33. E. Goli *et al.*, *Composites Part A: Applied Science and Manufacturing* **2020**, *130*, 1.
34. S. Vyas, E. Goli, X. Zhang, P. H. Geubelle, *Composites Science and Technology* **2019**, *184*, 107832.
35. I. D. Robertson *et al.*, *Nature* **2018**, *557*, 223.
36. S. Vyas, X. Zhang, E. Goli, P. H. Geubelle, *Composites Science and Technology* **2020**, *198*, 108303.
37. E. Goli, S. R. Peterson, P. H. Geubelle, *Composites Part B: Engineering* **2020**, *199*, 108306.
38. N. M. Chechilo, ENIKOLOP. NS, KHVILIVI. RY, *Doklady Akademii Nauk SSSR* **1972**, *204*, 1180.
39. N. M. Chechilo, N. S. Enikolopyan, *Dokl. Phys. Chem* **1975**, *221*, 392.
40. N. M. Chechilo, N. S. Enikolopyan, *Dokl. Phys. Chem* **1974**, *214*, 174.
41. N. M. Chechilo, N. S. Enikolopyan, *Dokl. Phys. Chem* **1976**, *230*, 840.
42. D. Bomze, P. Knaack, R. Liska, *Polymer Chemistry* **2015**, *6*, 8161.
43. C. Nason, J. A. Pojman, C. Hoyle, *Journal of Polymer Science Part A: Polymer Chemistry* **2008**, *46*, 8091.
44. M. S. Malik, S. Schlögl, M. Wolfahrt, M. Sangermano, *Polymers* **2020**, *12*, 2146.
45. Y. Xin, S. Xiao, Y. Pang, Y. Zou, *Progress in Organic Coatings* **2021**, *153*, 106149.
46. C. Ebner, J. Mitterer, J. Gonzalez-Gutierrez, G. Rieß, W. Kern, *Materials* **2021**, *14*, 743.
47. F. A. M. Abdul-Rasoul, A. Ledwith, Y. Yagci, *Polymer* **1978**, *19*, 1219.
48. A. Ledwith, *Pure and Applied Chemistry* **1979**, *51*, 159.
49. A. Ledwith, *Polymer* **1978**, *19*, 1217.
50. A. Mariani *et al.*, *Journal of Polymer Science, Part A: Polymer Chemistry* **2004**, *42*, 2066.
51. J. v. Crivello, *Journal of Polymer Science Part A: Polymer Chemistry* **2007**, *45*, 4331.
52. D. Bomze, P. Knaack, R. Liska, *Polymer Chemistry* **2015**, *6*, 8161.
53. N. Klikovits, P. Knaack, D. Bomze, I. Krossing, R. Liska, *Polymer Chemistry* **2017**, *8*, 4414.
54. H. Švajdlenková *et al.*, *RSC Advances* **2020**, *10*, 41098.
55. D. Bomze, P. Knaack, T. Koch, H. Jin, R. Liska, *Journal of Polymer Science, Part A: Polymer Chemistry* **2016**, *54*, 3751.
56. N. Klikovits, R. Liska, A. D'Anna, M. Sangermano, *Macromolecular Chemistry and Physics* **2017**, *218*, 1700313.
57. G. Hu *et al.*, *Materials* **2020**, *13*, 5838.
58. B. R. Groce, D. P. Gary, J. K. Cantrell, J. A. Pojman, *Journal of Polymer Science* **2021**, *59*, 1678.
59. M. Birkner, A. Seifert, S. Spange, *Polymer* **2019**, *160*, 19.
60. M. Sangermano, A. D'Anna, C. Marro, N. Klikovits, R. Liska, *Composites Part B: Engineering* **2018**, *143*, 168.
61. M. Sangermano, I. Antonazzo, L. Sisca, M. Carello, *Polymer International* **2019**, *68*, 1662.

62. A. D. Tran, T. Koch, P. Knaack, R. Liska, *Composites Part A: Applied Science and Manufacturing* **2020**, *132*, 105855.
63. A. D. Tran, T. Koch, R. Liska, P. Knaack, *Monatshefte fur Chemie* **2021**, *152*, 151.
64. J. v. Crivello, U. Varlemann, *ACS Symposium Series* **1997**, *673*, 82.
65. J. v. Crivello, U. Varlemann, *Journal of Polymer Science Part A: Polymer Chemistry* **1995**, *33*, 2463.
66. M. Fache, R. Auvergne, B. Boutevin, S. Caillol, *European Polymer Journal* **2015**, *67*, 527.
67. C. Noè *et al.*, *Progress in Organic Coatings* **2019**, *133*, 131.
68. A. Mariani *et al.*, *Journal of Polymer Science, Part A: Polymer Chemistry* **2004**, *42*, 2066.
69. J. A. Pojman, *Polymer Science: A Comprehensive Reference* **2012**, *4*, 957.
70. M. Sangermano, I. Antonazzo, L. Sisca, M. Carello, *Polymer International* **2019**, *68*, 1662.
71. E. Goli *et al.*, *Journal of Applied Polymer Science* **2019**, *136*, 47418.
72. D. Bomze, P. Knaack, R. Liska, *Polymer Chemistry* **2015**, *6*, 8161.
73. Y. Hu *et al.*, *Polymers for Advanced Technologies* **2018**, *29*, 1852.
74. A. Ruiz De Luzuriaga *et al.*, *Materials Horizons* **2016**, *3*, 241.
75. A. Cherdoud-Chihani, M. Mouzali, M. J. M. Abadie, *Journal of Applied Polymer Science* **1998**, *69*, 1167.
76. S. Malburet, D. Mauro, C. Noè, A. Mija, *RSC Advances* **2020**, 41954, doi:10.1039/d0ra07682a.
77. C. Noè *et al.*, *Macromolecular Materials and Engineering* **2021**, , 2100029.
78. N. G. Karsli, A. Aytac, *Composites Part B: Engineering* **2013**, *51*, 270.
79. A. Hassan, N. A. Rahman, R. Yahya, *Fibers and Polymers* **2012**, *13*, 899.
80. C. S. M. F. Costa, A. C. Fonseca, A. C. Serra, J. F. J. Coelho, *Polymer Reviews* **2016**, *56*, 362.
81. A. Etaati, S. Pather, Z. Fang, H. Wang, *Composites Part B: Engineering* **2014**, *62*, 19.
82. S. Ratim, N. N. Bonnia, N. S. Surip, *AIP Conference Proceedings* **2012**, *1455*, 131.
83. M. Indra Reddy, M. Anil Kumar, C. Rama Bhadri Raju, *Materials Today: Proceedings* **2018**, *5*, 458.
84. N. Saba, O. Y. Alothman, Z. Almutairi, M. Jawaid, *Construction and Building Materials* **2019**, *201*, 138.
85. V. Chaudhary, P. K. Bajpai, S. Maheshwari, *Journal of Natural Fibers* **2018**, *15*, 80.
86. A. S. J. Sekaran, K. P. Kumar, K. Pitchandi, **2015**, *38*, 1183.
87. R. Shrivastava, A. Telang, R. S. Rana, R. Purohit, *Materials Today: Proceedings* **2017**, *4*, 3477.
88. K. R. Sumesh, K. Kanthavel, V. Kavimani, *International Journal of Biological Macromolecules* **2020**, *150*, 775.
89. A. Genua *et al.*, *Polymers* **2020**, *12*, 2645.
90. ASTM, *Annual Book of ASTM Standards* **2014**, 1, doi:10.1520/D3039.

Fully biobased composites are successfully cured *via* "green" and fast frontal photopolymerization technique. Two different natural fiber fabrics made of cellulose and flax fibers are selected as reinforcing agents for a biobased epoxy resin deriving from vanillin alcohol. The thermo-mechanical properties of the composites increase as the fibre content increases confirming a good adhesion between the matrix and the fibre fabrics.

*C. Noè, M.Hakkarainen,, S. Malburet, A. Graillot, K.e Adekunle, M. Skrifvars, M. Sangermano**

Frontal-photopolymerization of fully biobased epoxy composites

ToC

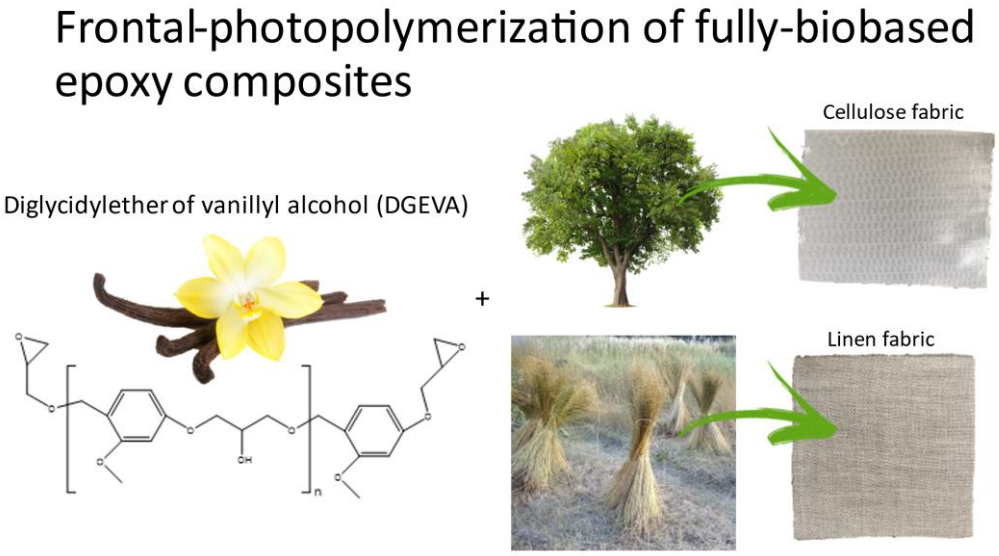

Supporting Information

Frontal-photopolymerization of fully biobased epoxy composites

*Camilla Noè, Minna Hakkarainen,, Samuel Malburet, Alain Graillot, Kayode Adekunle, Mikael Skrifvars, Marco Sangermano**

Figure 1S. DSC thermograms of DGEVA resin first and second run (a), DGEVA after RICFP curing first and second run (b).